Multiple Aerosol Unmixing by the Split Bregman Algorithm

Russell Warren[*]   *Stanley Osher*[**]   *Richard Vanderbeek*

EO-Stat Inc.   Department of Mathematics   US Army, ECBC
Chapel Hill, NC   UCLA, Los Angeles, CA   Aberdeen Proving Ground, MD

Abstract

For more than a decade the US government has been developing laser-based sensors for detecting, locating, and classifying aerosols in the atmosphere at safe standoff ranges. The motivation for this work is the need to discriminate aerosols of biological origin from interferent materials such as smoke and dust using the backscatter from multiple wavelengths in the long-range IR (LWIR) spectral region. Through previous work, algorithms have been developed for estimating the aerosol spectral dependence and concentration range-dependence from these data. The range-dependence is required for locating and tracking the aerosol plumes, and the backscatter spectral dependence is used for discrimination by a support vector machine classifier. Substantial progress has been made in these algorithms for the case of a single aerosol present in the lidar line-of-sight (LOS).

Often, however, mixtures of aerosols are present along the same LOS overlapped in range and time. Analysis of these mixtures of aerosols presents a difficult inverse problem that cannot be successfully treated by the methods used for single aerosols. Fortunately, recent advances have been made in the analysis of inverse problems using shrinkage-based L_1-regularization techniques. Of the several L_1-regularization methods currently known, the split Bregman algorithm is straightforward to implement, converges rapidly, and is applicable to a broad range on inverse problems including our aerosol unmixing. In this paper we show how the split Bregman algorithm can successfully resolve LWIR lidar data containing mixtures of bioaerosol simulants and interferents into their separate components. The individual components then can be classified as bio- or non-bio aerosol by our SVM classifier. We illustrate the approach through data collected in field tests over the past several years using the US Army FAL sensor in testing at Dugway Proving Ground, UT.

Report Documentation Page		*Form Approved* *OMB No. 0704-0188*

Public reporting burden for the collection of information is estimated to average 1 hour per response, including the time for reviewing instructions, searching existing data sources, gathering and maintaining the data needed, and completing and reviewing the collection of information. Send comments regarding this burden estimate or any other aspect of this collection of information, including suggestions for reducing this burden, to Washington Headquarters Services, Directorate for Information Operations and Reports, 1215 Jefferson Davis Highway, Suite 1204, Arlington VA 22202-4302. Respondents should be aware that notwithstanding any other provision of law, no person shall be subject to a penalty for failing to comply with a collection of information if it does not display a currently valid OMB control number.

1. REPORT DATE **MAY 2011**	2. REPORT TYPE	3. DATES COVERED **00-00-2011 to 00-00-2011**
4. TITLE AND SUBTITLE **Multiple Aerosol Unmixing by the Split Bregman Algorithm**		5a. CONTRACT NUMBER
		5b. GRANT NUMBER
		5c. PROGRAM ELEMENT NUMBER
6. AUTHOR(S)		5d. PROJECT NUMBER
		5e. TASK NUMBER
		5f. WORK UNIT NUMBER
7. PERFORMING ORGANIZATION NAME(S) AND ADDRESS(ES) **University of California, Los Angeles (UCLA),Department of Mathematics,Los Angeles,CA,90095**		8. PERFORMING ORGANIZATION REPORT NUMBER
9. SPONSORING/MONITORING AGENCY NAME(S) AND ADDRESS(ES)		10. SPONSOR/MONITOR'S ACRONYM(S)
		11. SPONSOR/MONITOR'S REPORT NUMBER(S)

12. DISTRIBUTION/AVAILABILITY STATEMENT
Approved for public release; distribution unlimited

13. SUPPLEMENTARY NOTES

14. ABSTRACT

For more than a decade the US government has been developing laser-based sensors for detecting, locating, and classifying aerosols in the atmosphere at safe standoff ranges. The motivation for this work is the need to discriminate aerosols of biological origin from interferent materials such as smoke and dust using the backscatter from multiple wavelengths in the long-range IR (LWIR) spectral region. Through previous work, algorithms have been developed for estimating the aerosol spectral dependence and concentration range-dependence from these data. The range-dependence is required for locating and tracking the aerosol plumes, and the backscatter spectral dependence is used for discrimination by a support vector machine classifier. Substantial progress has been made in these algorithms for the case of a single aerosol present in the lidar line-of-sight (LOS). Often, however, mixtures of aerosols are present along the same LOS overlapped in range and time. Analysis of these mixtures of aerosols presents a difficult inverse problem that cannot be successfully treated by the methods used for single aerosols. Fortunately, recent advances have been made in the analysis of inverse problems using shrinkage-based L1-regularization techniques. Of the several L1-regularization methods currently known, the split Bregman algorithm is straightforward to implement, converges rapidly, and is applicable to a broad range on inverse problems including our aerosol unmixing. In this paper we show how the split Bregman algorithm can successfully resolve LWIR lidar data containing mixtures of bioaerosol simulants and interferents into their separate components. The individual components then can be classified as bio- or non-bio aerosol by our SVM classifier. We illustrate the approach through data collected in field tests over the past several years using the US Army FAL sensor in testing at Dugway Proving Ground, UT.

15. SUBJECT TERMS

16. SECURITY CLASSIFICATION OF:			17. LIMITATION OF ABSTRACT	18. NUMBER OF PAGES	19a. NAME OF RESPONSIBLE PERSON
a. REPORT **unclassified**	b. ABSTRACT **unclassified**	c. THIS PAGE **unclassified**	**Same as Report (SAR)**	**17**	

1. Introduction

This work describes a generalization of previous research[1] on developing efficient algorithms for estimating the parameters of optically thin aerosols in the atmosphere using data from rapidly tuned multiple-wavelength long wave infrared (LWIR) lidar. The motivation for this work remains the same: the need for detecting, locating, tracking, and discriminating atmospheric aerosols at safe standoff ranges using time-series data collected at a discrete set of CO_2 laser wavelengths. Our earlier work considered a single aerosol material producing a backscatter enhancement over that from the natural atmosphere. The goals were to detect and track the aerosol by means of estimates of the range-dependence of the concentration, and to discriminate potentially harmful aerosols—particularly those of biological origin—from interferents such as smoke and dust by means of the spectral dependence of the backscatter. State-of-the-art support vector machine (SVM) classifiers have been developed for this discrimination.

Often, however, mixtures of aerosols are present along the same lidar line-of-sight overlapped in range and time. For example, it is quite possible to have a biological or chemical agent release from a munition accompanied by dust and other byproducts of the explosive release. Those extra materials can distort the spectral dependence of the threat material and degrade the ability of the sensor to correctly identify the threat. The analysis of aerosol mixtures presents a difficult inverse problem that cannot be successfully treated by the methods used previously for single materials.

Fortunately, recent advances have been made in the analysis of inverse problems using shrinkage-based L_1-regularization techniques. We focus here on the split Bregman algorithm[2] because it is straightforward to implement, converges rapidly, and is applicable to a broad range of inverse problems including our aerosol unmixing. In this paper we show how the split Bregman algorithm can successfully resolve LWIR lidar data containing mixtures of bioaerosol simulants and interferents into their separate components. The individual components then can be classified as bio- or non-bio aerosol by our SVM classifier.

The use of Bregman iteration to solve difficult L_1-estimation problems efficiently was described by Yin *et al*.[3] In that paper they showed the equivalence of Bregman iteration to the augmented Lagrangian method for the minimization of convex functions with linear constraints. In a subsequent paper, Goldstein and Osher [2] showed that Bregman iteration could be efficiently implemented by splitting the original combination of L_1 and L_2 optimizations over a single variable into two separate minimizations; one over a differentiable quadratic component, and a second over a non-differentiable L_1-norm

---

[1] R. E. Warren, R. G. Vanderbeek, A. Ben-David, and J. L. Ahl, *Simultaneous estimation of aerosol cloud concentration and spectral backscatter from multiple-wavelength lidar data*, Appl. Optics, 47, pp 4309-4320, 2008.

[2] T. Goldstein and S. Osher, *The split Bregman method for L1-regularized problems.* SIAM J. Imaging Sci., 2(2):323-343, 2009. ISSN 1936-4954.

[3] W. Yin, S. Osher, D. Goldfarb, and J. Darbon, *Bregman iterative algorithms for l1-minimization with application to compressed sensing*, SIAM J. Imaging Sci., vol. 1, pp 143-168, 2008.

component with an objective function that could be solved in closed form by shrinkage. This is the origin of the term split Bregman. Subsequently,[4,5] it was recognized that their splitting algorithm could be interpreted from a Lagrangian and penalty standpoint (augmented Lagrangian) analogous to that described in [3]. It is this augmented Lagrangian interpretation of split Bregman that we follow here. For a comprehensive analysis of the interrelations between Bregman iteration, augmented Lagrangians, split Bregman, and other techniques, see the review by Esser.[6]

In our treatment of single aerosol estimation, we gave a rather detailed discussion of the lidar measurement and preprocessing needed to remove the effects of the natural atmosphere and to deconvolve the long CO_2 transmitter pulse waveforms. Those discussions pertain here without any modification. We therefore concentrate on the problem of generalizing the estimation to multiple aerosols by use of the split Bregman method. Accordingly, section 2 provides a brief summary of the advantages of L_1-regularization over the more traditional L_2 method, and more particularly, how this newer, more robust method can be implemented efficiently through split Bregman. Section 3 describes how the multi-aerosol estimation is formulated as a dual application of the basic split Bregman algorithm. In section 4 we give some examples of processing aerosol mixture data from both simulated and actual release data collected by the US Army FAL sensor during testing at Dugway Proving Ground, UT. Section 5 summarizes and concludes.

2. L_1-Regularization of Inverse Problems by the Split Bregman Method

It is well known that inverse problems such as the retrieval of signals observed after some smoothing operation such as blurring are ill-posed in the sense that small changes in the data due to noise, for example, can have large effects on the solution. Otherwise stated, many different solutions are compatible with the same data. Since most of these "solutions" are wildly oscillatory, and therefore not physically meaningful, some sort of regularization is required to produce useful results. Historically, L_2-regularization has been used in the context of least-squares estimation since it is easy to implement through ridge regression. Although stabilizing the solution, ridge regression tends to be unselective in the features it suppresses and can lead to severely biased results.

As noted above, more recent alternatives to L_2-regularization have replaced the quadratic regularization term in the objective function with an L_1-norm regularizing term. This has the effect of selectively removing features in the estimate that produce the large fluctuations associated with direct inversion without regularization. This selectivity gives L_1 estimates a sparse representation in an appropriate basis set. The downside of L_1-

[4] X. Tai and C. Wu, *Augmented Lagrangian method, dual methods and split Bregman iteration for ROF model*, Scale Space and Variational Methods in Computer Vision: Lecture Notes in Computer Science, vol. 5567/2009, pp 502-513, 2009.

[5] Y. Gui-Bo and X. Xiaohui, *Split Bregman for large scale fused Lasso*, J. Computational Statistics and Data Analysis, vol. 55, no. 4, April, 2011.

[6] E. Esser, *Applications of Lagrangian-based alternating direction methods and connections to split Bregman*, UCLA CAM report 09-31, 2009.

regularization has been the loss of differentiability of the objective function making implementation more difficult than L_2.

As noted above, the new class of shrinkage-based inversion methods such as split Bregman largely overcomes the computational limitations of L_1-regularization. To illustrate the advantages of L_1 over L_2 we compare them on a simple one-dimensional simulated example. Our objective is to minimize the functionals $J_1(u)$ and $J_2(u)$:

$$\hat{u}_{1,2} = \arg\min_u J_{1,2}(u),$$

$$J_1(u) = \frac{1}{2}\|Ku - f\|_2^2 + \lambda\|u\|_1,$$

$$J_2(u) = \frac{1}{2}\|Ku - f\|_2^2 + \frac{\mu}{2}\|u\|_2^2,$$

where $J_{1,2}$ are the sum of a quadratic term quantifying the fidelity of the linear model Ku to the data f and the second terms are regularizers using the L_1 and L_2 norms, respectively:

$$\|u\|_1 \equiv \sum_k |u_k|, \quad \|u\|_2 \equiv \left[\sum_k |u_k|^2\right]^{1/2}.$$

We assume the model operator K and the data to be known. The scalar coefficients λ and μ are set heuristically to balance the conflicting needs for fitting the model and solution smoothness.

For concreteness we modeled u as the sum of two narrow Gaussian functions given by

$$u(x) = \exp\left[-(x+0.1)^2/0.001\right] + \exp\left[-(x-0.1)^2/0.001\right],$$

and shown in Figure 1 sampled uniformly over 1000 points between -2 and 2. The data f were created by blurring u with a Toeplitz matrix

$$K_{nm} = \frac{1}{50}r^{|n-m|},$$

with $r = 0.99$, and adding zero-mean independently distributed (pseudo-)random normal noise with standard error $\sigma = 0.004$:

$$f_n = \sum_m K_{nm}u_m + q_n,$$

$$q_n \,\square\, N\left(0, \sigma^2\right).$$

The simulated data are shown in Figure 1 together with the L_2 regression estimate at the value $\mu = 0.015$, and the L_1 estimate computed by the split Bregman method defined below also using $\lambda = 0.015$. We note the L_2 estimate is unable to resolve the peaks, whereas the L_1 estimate gives a clean separation of the two components.
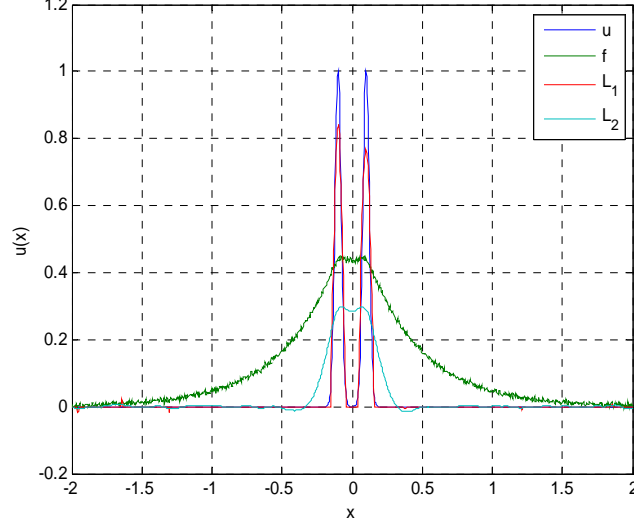

Fig. 1 Data and estimates from the narrow Gaussian example.

The objective function J_1 is non-smooth because of the L_1-norm regularization term. This makes the optimization over u difficult by the usual calculus-based methods. The basic idea of split Bregman is to introduce additional variables into the J_1 objective function that will allow a convenient separation of the minimizations over the quadratic (smooth) data term

$$H(u) = \frac{1}{2}\|Ku - f\|_2^2$$

and the non-smooth regularization term $\|u\|_1$. This is done in two steps. First, the unconstrained problem $\arg\min_u H(u) + \|u\|_1$ is replaced by the equivalent constrained problem

$$\arg\min_u H(u) + \|d\|_1 \text{ such that } u = d.$$

Second, the constraint $u = d$ is enforced by adding a Lagrange multiplier term and an additional quadratic penalty term to get the Lagrangian

$$L(u,d,b) = H(u) + \|d\|_1 + \lambda\langle b, u - d\rangle + \frac{\lambda}{2}\|u - d\|_2^2, \tag{1}$$

where b is the Lagrange multiplier vector, $\langle a,b \rangle$ denotes the inner product of vectors a and b, and λ is a positive regularization parameter. In this formulation, L assumes the form of an augmented Lagrangian [4, 5] to be minimized for u and d, and maximized for the dual variable b. In the appendix the derivation of this saddle point optimization is sketched. The resulting algorithm is given as Algorithm 1. The function $S_\lambda(x)$ appearing in Algorithm 1 is the shrinkage operator that plays a key role in the success of the method by promoting sparseness in the solution through shrinking input values toward zero. S is defined as

$$S_\lambda(x) \equiv \begin{cases} x - \lambda, x > \lambda \\ 0, -\lambda \le x \le \lambda \\ x + \lambda, x < -\lambda \end{cases}. \tag{2}$$

Initialization: $d^0 = b^0 = 0, k = 0, \|\Delta u\|_2 = 1$

while $\|\Delta u\|_2 > \varepsilon$,

$\qquad u^{k+1} = \left(K^T K + \lambda I \right)^{-1} \left(K^T f + \lambda \left(d^k - b^k \right) \right),$

$\qquad d^{k+1} = S_\lambda \left(u^{k+1} + b^k \right),$

$\qquad b^{k+1} = b^k + u^{k+1} - d^{k+1},$

$\qquad \Delta u = u^{k+1} - u^k,$

$\qquad k \rightarrow k + 1,$

end

Algorithm 1 Split Bregman algorithm.

---

3. Multi-Aerosol Split Bregman Algorithm

In this section we generalize the basic split Bregman method described in section 2 to treat the aerosol unmixing problem for multiple aerosols within a single lidar line-of-sight. Our starting point is the $M \times N$ matrix $\{G_{jk}\}$ that represents the range-resolved lidar data at a single time-step after the preprocessing to remove the natural aerosol backscatter and transmitter pulse effects as described in [1]. The row index of G, $1 \le j \le M$, labels the wavelength, and the column index, $1 \le k \le N$, labels the digitized range-cell. We model G as the additive combination of the aerosol backscatter from L materials

$$G_{jk} = \sum_{l=1}^{L} \rho_{jl} C_{lk} + n_{jk},$$

6

where ρ_{jl} are the spectral backscatter variables as a function of wavelength and material, and C_{lk} are the concentration variables as a function of material and range-cell. The variables n_{jk} represent zero-mean additive noise. As discussed in [1], to lead to an identifiable model we must constrain ρ and C for each material. We adopt the choice made in [1] of requiring that $C_{lk} \geq 0$, $\rho_{jl} \geq 0$, and the backscatter estimates be unit vectors for each material: $\sum_j \rho_{jl}^2 = 1$.

Our goal is to resolve G into L aerosol components using a generalization of the L_1-regularized split Bregman method. To that end we perform the splitting by introducing the constrained versions of ρ and C, d and e, that carry the L_1-norm regularizations, and Lagrange dual variables b and c that enforce the constraints $\rho = d$, and $C = e$ within an augmented Lagrangian framework. Setting the data fidelity term

$$H(\rho,C) = \frac{1}{2}\sum_{j,k}\left[G_{jk} - \sum_{l=1}^{L}\rho_{jl}C_{lk}\right]^2,$$

we have the augmented Lagrangian

$$L(\rho,C,d,e,b,c) = H(\rho,C) + \|d\|_1 + \|e\|_1 + \lambda_\rho\langle b, \rho-d\rangle + \lambda_C\langle c, C-e\rangle$$
$$+ \frac{\lambda_\rho}{2}\|\rho-d\|_2^2 + \frac{\lambda_C}{2}\|C-e\|_2^2,$$

to be minimized over ρ, C, d, e, and maximized over b and c such that $\rho \geq 0$, $C \geq 0$, and $\|\rho\|_2 = 1$ for each material. The parameters $\lambda_\rho > 0$ and $\lambda_C > 0$ control the balance between fitting errors and parameter smoothness, and are set heuristically using a combination of simulated and test data.

As in the case of the basic split Bregman algorithm, the multi-aerosol augmented Lagrangian leads to a saddle point solution that iterates between concentration and backscatter using three iterated steps for each component given current estimates of the other. The steps for backscatter are:

1. $\rho^{n+1} = \arg\min_{\rho}\left[H\left(\rho,C^n\right) + \lambda_\rho\langle b^n, \rho-d^n\rangle + \frac{\lambda_\rho}{2}\|\rho-d^n\|_2^2\right]$, $\quad \rho^{n+1} \to |\rho^{n+1}|/\|\rho^{n+1}\|$

2. $d^{n+1} = \arg\min_{d}\left[\|d\|_1 + \lambda_\rho\langle b^n, \rho^{n+1}-d\rangle + \frac{\lambda_\rho}{2}\|\rho^{n+1}-d\|_2^2\right]$

3. $b^{n+1} = b^n + \rho^{n+1} - d^{n+1}$

7

Because of the introduction of *d*, the problem splits into three easily solved components: the first step is solved by calculus, the second step is solved by shrinkage, and the third step is explicit.

The corresponding steps for concentration are:

1. $C^{n+1} = \arg\min_C \left[H(\rho^{n+1}, C) + \lambda_C \left\langle c^n, C - e^n \right\rangle + \frac{\lambda_C}{2} \left\| C - e^n \right\|_2^2 \right], \quad C^{n+1} \to \max\left(C^{n+1}, 0 \right)$

2. $e^{n+1} = \arg\min_e \left[\left\| e \right\|_1 + \lambda_C \left\langle c^n, C^{n+1} - e \right\rangle + \frac{\lambda_C}{2} \left\| C^{n+1} - e \right\|_2^2 \right]$

3. $c^{n+1} = c^n + C^{n+1} - e^{n+1}$

Algorithm 2 gives the resulting unmixing algorithm. The function S_λ is the shrinkage operator (2). The recursions in Algorithm 2 are initialized by prior estimates of the backscatter, if available, or randomly. Typically, 10 iterations are enough to give good results.

4. Numerical Examples

In this section we illustrate the multi-aerosol unmixing algorithm on simulated and actual release data collected by the US Army FAL (Frequency Agile Lidar) sensor. The calculations were done by implementing Algorithm 2 in MATLAB on a PC. The simulated FAL data were created by injecting two overlapping aerosol plumes having Gaussian range-dependence both centered at 1.5 km with width 50 m into background FAL data sets. Those sets consisted of transmitted pulse waveforms and received laser backscatter from the natural atmosphere as a function of time-step, wavelength index, and range-cell. The two injected plumes represent a bioaerosol simulant (bacillus BG) and interferent (kaolin dust). The simulant plume was injected between time-steps 200 and 600, and the interferent between time-steps 400 and 800. A randomly varying peak concentration was created from a first-order AR model. The purpose of the simulator was to generate data for overall algorithm performance verification including background removal and transmitter pulse deconvolution. Because those operations are not relevant to the present discussion, we focus on the comparison of the input concentration and backscatter waveforms with the estimates from the split Bregman algorithm after data preprocessing.

Figure 2 shows the concentration estimates from the unmixing algorithm with regularization parameters set at $\lambda_\rho = \lambda_C = 0.05$. The plots show the bioaerosol estimates (left) and interferent (right) versus time-step and range. The calculation was initialized using the mean of the backscatter spectral estimates used to train our support vector machine classifier for the bioaerosol and interferent classes.

8

Figure 3 compares the input and estimated peak concentration over range as a function of time-step for the bioaerosol (top) and interferent (bottom). We see that the estimates track the input throughout the run including the plume overlap region. For comparison, Figure 4 plots the peak concentration estimates from a previous algorithm based on using backscatter mean spectra as priors in a Bayesian scheme. Since the prior as well as data densities were chosen to be Gaussian, the Bayes approach in effect is doing quadratic norm processing. Although giving good results when the plumes are separated in time, this processor fails to produce good material separation in the overlap region.

Initialize ρ^0 through prior estimates or randomly.
$D\rho = 1, \rho_{old} = 0$
while $D\rho > \varepsilon$

  $e^0 = c^0 = d^0 = b^0 = 0, n = 0, C^0 = 0, \|\Delta C\|_2 = 1$

  while $\|\Delta C\|_2 > \varepsilon$

    $C^{n+1} = \left(\rho^{nT}\rho^n + \lambda_C I\right)^{-1}\left(G^T\rho^n + \lambda_C\left(e^n - c^n\right)\right),$

    $C^{n+1} \to \max\left(C^{n+1}, 0\right),$

    $e^{n+1} = S_\lambda\left(C^{n+1} + c^n\right),$

    $c^{n+1} = c^n + C^{n+1} - e^{n+1},$

    $\Delta C = C^{n+1} - C^n,$

    $n \to n+1,$

  end

  $\hat{C} = C^{n+1}, \|\Delta\rho\|_2 = 1, n = 0$

  while $\|\Delta\rho\|_2 > \varepsilon$

    $\rho^{n+1} = \left(\hat{C}\hat{C}^T + \lambda_\rho I\right)^{-1}\left(G\hat{C}^T + \lambda_\rho\left(d^n - b^n\right)\right),$

    $\rho^{n+1} \to \left|\rho^{n+1}\right|/\left\|\rho^{n+1}\right\|_2,$

    $d^{n+1} = S_\lambda\left(\rho^{n+1} + b^n\right),$

    $b^{n+1} = b^n + \rho^{n+1} - d^{n+1},$

    $\Delta\rho = \rho^{n+1} - \rho^n,$

    $n \to n+1,$

  end

  $\hat{\rho} = \rho^{n+1}, D\rho = \|\hat{\rho} - \rho_{old}\|_2, \rho_{old} = \hat{\rho}$

end

Output $\hat{\rho}$ and $\hat{C}$

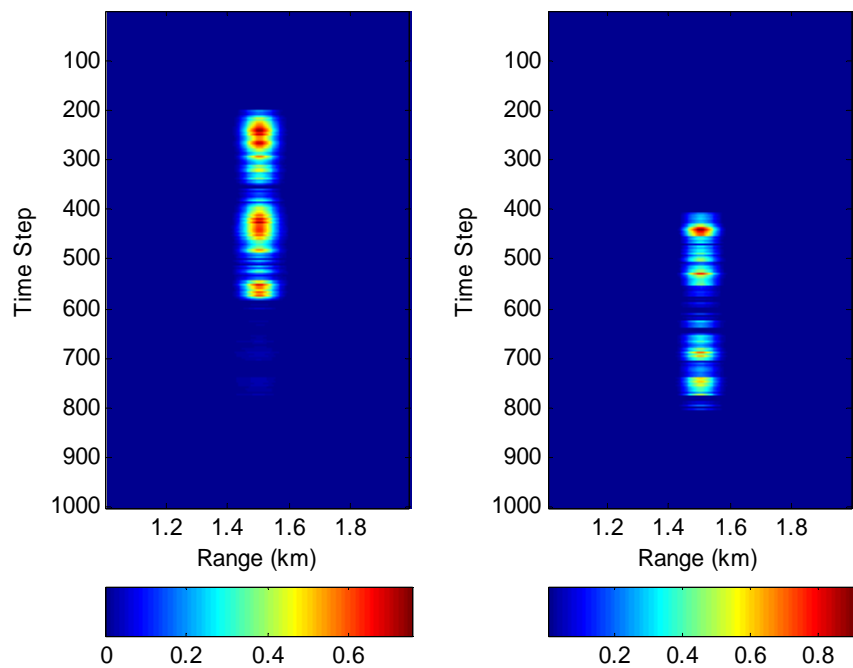**Algorithm 2** Split Bregman algorithm for multi-aerosol unmixing.

Fig. 2 Concentration estimates (bioaerosol left and interferent right) from simulated data example.
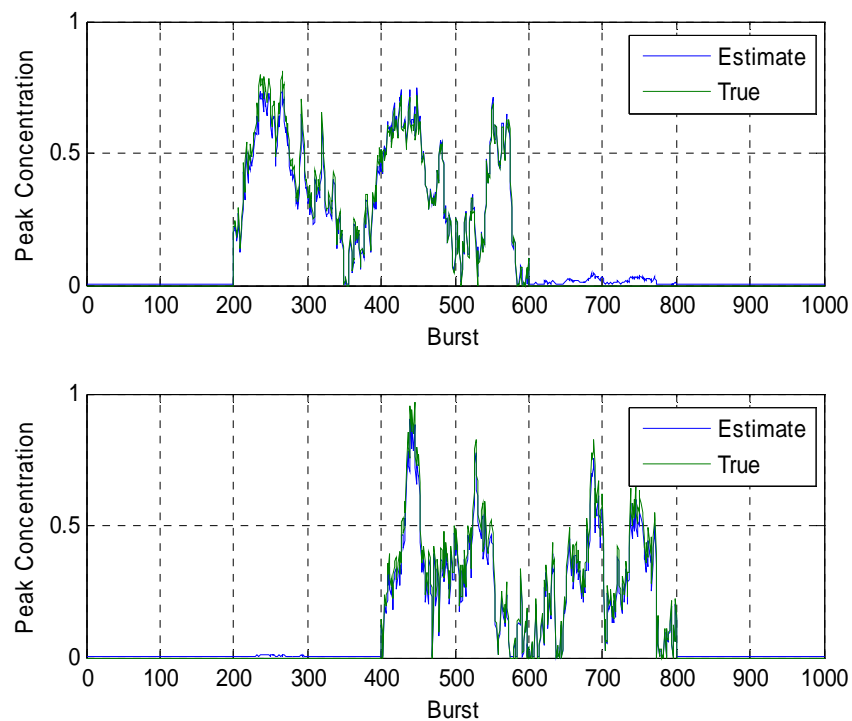
Fig. 3 Split Bregman peak concentration estimates for bioaerosol (top) and interferent (bottom).

Figures 5 and 6 compare the concentration range-dependence (true and estimated) and backscatter wavelength dependence at time steps 300 and 700 for the bioaerosol and interferent, respectively. The results suggest that the split Bregman unmixing can provide both low bias and low variance estimates.
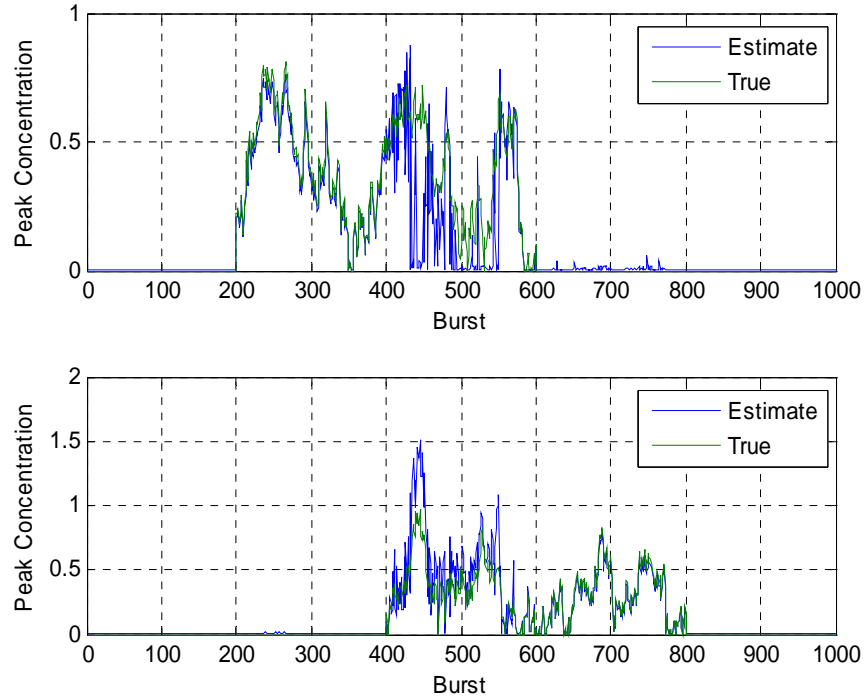

Fig. 4 Peak concentration estimates using a Bayes (quadratic norm) approach.

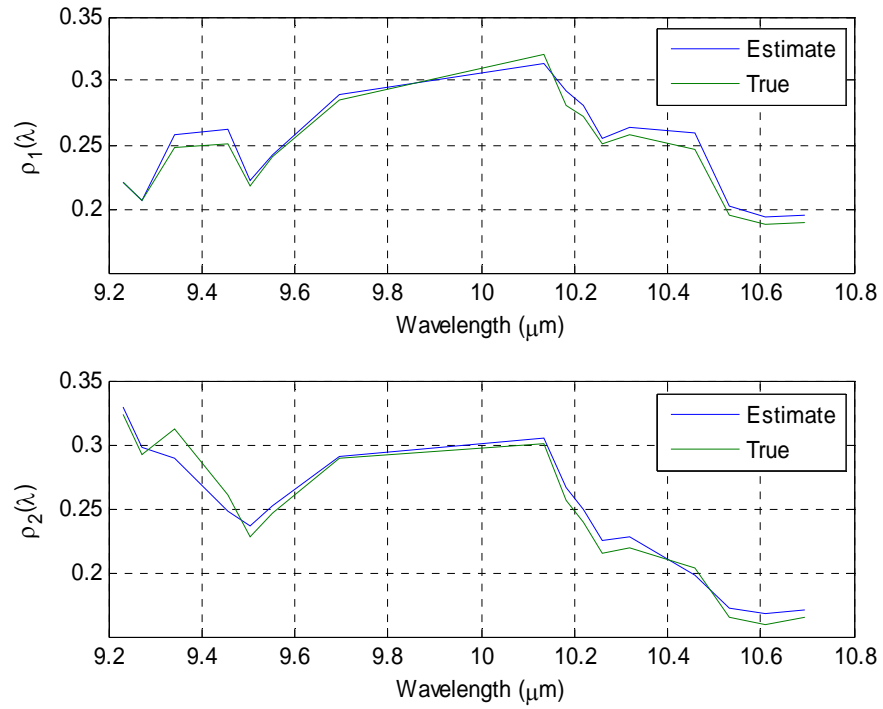**Fig. 5** Concentration range-dependence for bioaerosol (top) and interferent (bottom).

Fig. 6 Backscatter wavelength-dependence for bioaerosol (top) and interferent (bottom).

As an example of processing FAL data from a mixture of aerosols, we consider the partially overlapped release TD4065 of Florida BG (a bioaerosol simulant) and Kuwait dust on May 31, 2008 in the Joint Ambient Breeze Tunnel (JABT) at Dugway Proving Ground, UT. The FAL sensor was located about 1.2 km from the entrance to the JABT. The bioaerosol was released between time-steps 100-476, and the dust between times 261-633. Data collected during the first 100 time-steps were used to estimate the backscatter from the natural atmosphere. The aerosols were injected near the far end of the tunnel, and drawn toward the front of the tunnel by large fans where they were exhausted.

Figure 7 shows the concentration estimates from the unmixing algorithm on these data with the bioaerosol (dust) plotted on the left (right). We see the initial localized aerosol appearing at the indicated beginning of the releases. The subsequent time-steps show the plumes expanding to fill the space between the injection and extraction locations. Figure 8 plots the peak concentration over range with the bioaerosol (dust) shown at the top (bottom). We see a clean separation of the two aerosol components in these figures.

The estimates of aerosol backscatter are plotted in Figure 9 as a function of time-step and wavelength index for the 16 wavelengths used in these tests. Up to time-step 100 we see only the random unit vectors produced by the algorithm in the absence of aerosol. After the bioaerosol release (shown on the left) the estimates show a consistent structure, although they are rather noisy between time-steps 300-450 because of low concentration levels. The corresponding dust backscatter estimates (shown on the right) also show a consistent structure throughout the dust release.
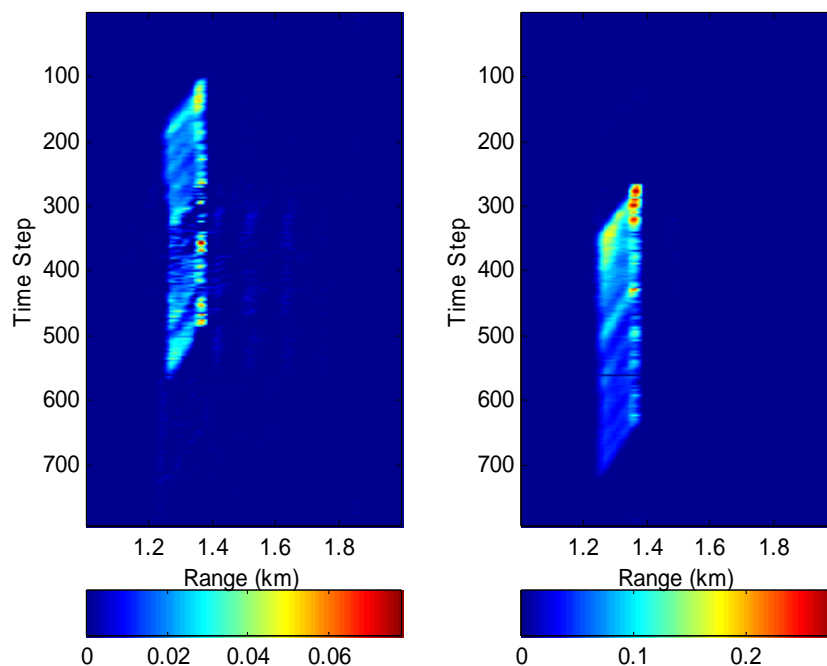

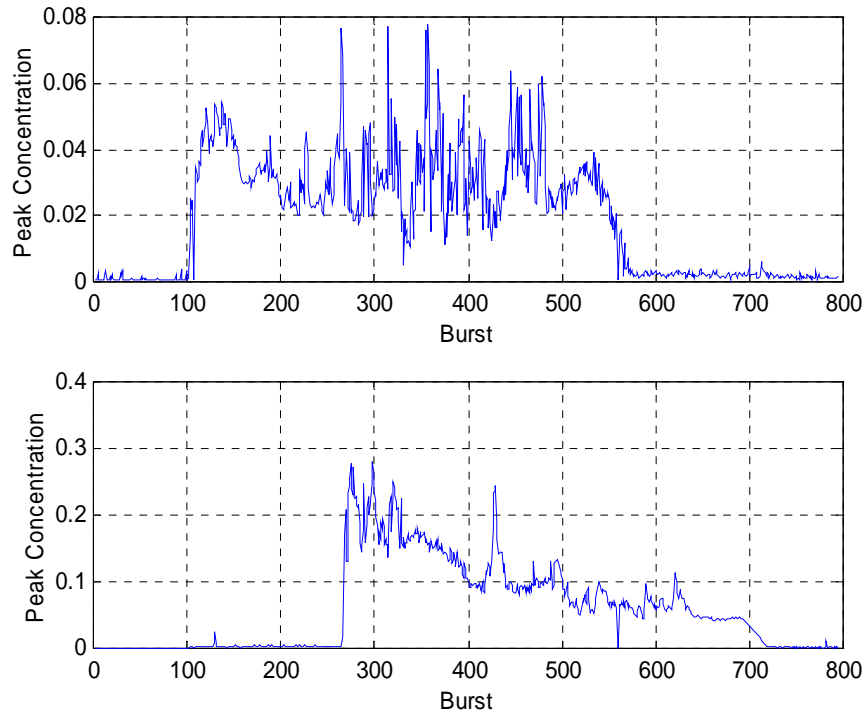**Fig. 7** Concentration estimates (bioaerosol left and dust right) from release TD4065.

13

Fig. 8 Peak concentration estimates for bioaerosol (top) and dust (bottom) from TD4065.
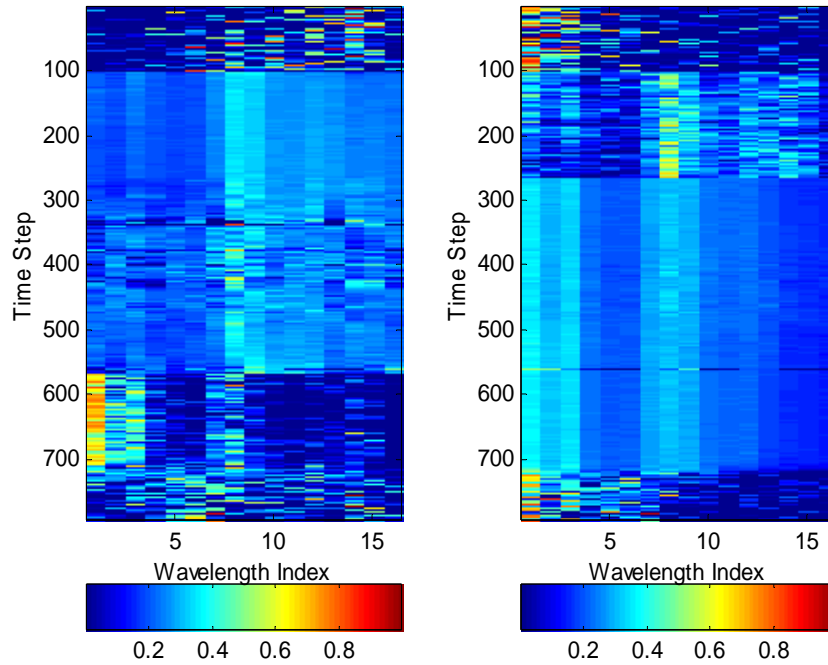

Fig. 9 Backscatter estimates for bioaerosol (left) and dust (right) for TD4065.

Finally, the aerosol classifier, a least-squares support vector machine (LS-SVM) classifier,[7] was applied to the backscatter estimates. Our classifier consists of a three-class discriminator for bioaerosol, interferent, and null classes. The latter class was included to allow the classifier to perform a detection function by rejecting spectral patterns that look like neither bioaerosol nor interferent. Three binary classifiers were trained by the 1-versus-rest method for discriminating samples from each class against the pooled alternatives. At each time-step the class whose classifier has the highest decision function value is chosen. Backscatter estimates from both material components were processed this way, and the results for the decision functions are plotted in Figure 10. The results indicate that the classifier recognized both materials at the correct times during the partially overlapped releases.
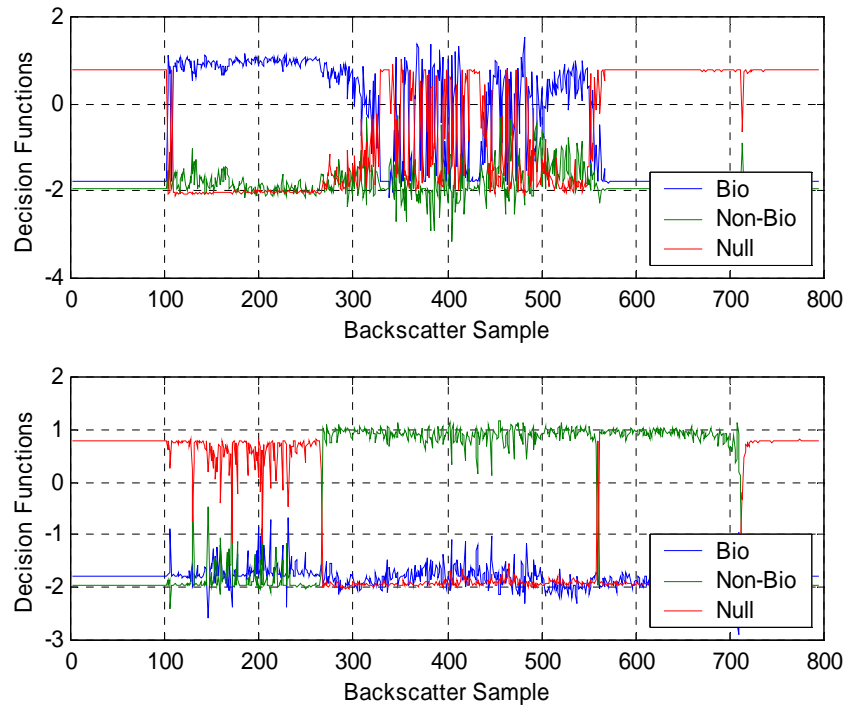

Fig. 10 LS-SVM decision functions for bioaerosol (top) and interferent (bottom) for TD4065.

5. Summary and Conclusions

The unmixing of elastic backscatter data from multi-wavelength, range-resolved lidar for aerosol mixtures has defied solution by traditional regularization methods using quadratic smoothing constraints. A new shrinkage-based L_1-regularization method for linear inverse problems, the split Bregman algorithm, has been successfully applied to the aerosol unmixing problem. It was illustrated here on simulated and actual aerosol

---

[7] J. A. K. Suykens, T.Van Gestel, J. De Brabanter, B. De Moor, and J. Vandwalle, *Least Squares Support Vector Machines,* World Scientific, 2002.

mixture release data collected by US Army personnel in field testing at Dugway proving Ground, UT using the rapidly tuned FAL sensor.

The capability of resolving data from mixtures of aerosols into their backscatter and concentration components is important to the success of standoff sensors for biological detection in realistic operating environments where interferent materials such as smoke and dust will usually be present. Failure to correctly perform this unmixing can lead to increased misclassifications that degrade the usefulness of potential sensors employing active detection.

Other possible standoff sensing applications of this unmixing technique include (1) the analysis of lidar data from chemical releases where the agent can have both vapor and aerosol phases and interferent materials can include byproducts of an explosive release, and (2) the use of thermal imaging sensors operating in the long wave infrared spectra region.

Appendix—Augmented Lagrangian Derivation of Split Bregman

Given the augmented Lagrangian function $L(u,d,b)$ in (1), we wish to find a saddle point $(u*,d*,b*)$ such that[8]

$$L(u*,d*,b) \le L(u*,d*,b*) \le L(u,d,b*).$$

We solve this saddle point problem by iterating between primal and dual optimizations:

$$(u^{k+1},d^{k+1}) = \arg\min_{u,d} L(u,d,b^k) \quad \text{(primal)}$$
$$b^{k+1} = b^k + u^{k+1} - d^{k+1} \quad \text{(dual)}$$

For the primal minimizations holding the dual variable b fixed, we note that because of the introduction of the d variables, the optimization over u can be done for fixed d by differentiation:

$$\frac{\partial L(u,d,b)}{\partial u} = K*(Ku - f) + \lambda b + \lambda(u - d)$$

to get

$$u^{k+1} = (K*K + \lambda I)^{-1}(K*f + \lambda(d^k - b^k)). \qquad \text{(A-1)}$$

---

[8] This sketch follows the split Bregman treatment given by Y. Gui-Bo and X. Xiaohui, "Split Bregman method for large scale fused Lasso*," J. Comp. Stat. & Data Analysis,* Vol. 55, No. 4, April 2011.

Likewise, although the *d* variable optimization is still non-smooth, it is very easy to solve by shrinkage for given *u* and *b*:

$$d^{k+1} = S_\lambda \left(u^{k+1} + b^k \right), \qquad\qquad\qquad \text{(A-2)}$$

where the shrinkage function S_λ is given by (2). Steps A-1 and A-2 can be iterated for fixed b^k, but we find it more efficient (usually) to perform them only once.